

Entropy of vortex cores near the superconductor-to-insulator transition in an underdoped cuprate

C. Capan, K. Behnia

Laboratoire de Physique Quantique(UPR5-CNRS), ESPCI, 10 Rue Vauquelin, F-75005 Paris, France

J. Hinderer, A. G. M. Jansen

Grenoble High Magnetic Field Laboratory(CNRS-MPI), BP 166, F- 38042 Grenoble , France

W. Lang

Institut für Materialphysik, Universität Wien, Boltzmannngasse 5 A-1090 Wien, Austria

C. Marcenat, C. Marin and J. Flouquet

DRFMC/SPSMS, Commissariat à l'Energie Atomique, F-38042 Grenoble, France

(October 10, 2001)

We present a study of Nernst effect in underdoped $La_{2-x}Sr_xCuO_4$ in magnetic fields as high as 28T. At high fields, a sizeable Nernst signal was found to persist in presence of a field-induced non-metallic resistivity. By simultaneously measuring resistivity and the Nernst coefficient, we extract the entropy of vortex cores in the vicinity of this field-induced superconductor-insulator transition. Moreover, the temperature dependence of the thermo-electric Hall angle provides strong constraints on the possible origins of the finite Nernst signal above T_c , as recently discovered by Xu *et al.* [1].

An intriguing case of vicinity between superconducting and insulating ground states occurs in the underdoped cuprates [2]. Various investigations have shown that reducing the density of charge carriers [3] or introducing disorder [4] or applying a magnetic field [2] leads to the replacement of the superconductor with an insulator. The latter route (i.e. the field-driven superconductor-to-insulator transition) raises many unanswered questions, including the possible existence of vortices with insulating cores. The structure of the vortex core in a doped Mott insulator has been the subject of numerous theoretical studies [5–7]. On the experimental side, recent neutron scattering experiments on $La_{2-x}Sr_xCuO_4$ (LSCO) have revealed the existence of a dynamic magnetic order associated with the vortex state which evolves towards a static order in the underdoped regime [8]. Meanwhile, Scanning Tunnelling Microscopy (STM) has proved to be a direct source of information on the electronic spectrum inside the vortices, and have detected finite-energy bound states in the vortex cores of optimally-doped cuprates [9,10]. Until now, however, experimental exploration of field-induced superconductor-to-insulator transition has been limited to resistivity measurements [2,11].

In this letter, we report on the evolution of the Nernst coefficient in underdoped LSCO in the vicinity of the superconductor-to-insulator transition. Nernst effect, the generation of a transverse electric field by a longitudinal thermal gradient in a magnetic field, has been an instructive probe of vortex movement in the mixed state of high- T_c superconductors in early 1990s [12]. Recently, Xu *et al.* [1] reported the existence of a sizeable Nernst signal above T_c over a broad temperature range in underdoped LSCO. They argued that, due to the cancellation of transverse currents generated by the thermal

gradient and the electric field in presence of a magnetic field, the quasiparticle contribution to the Nernst signal should be negligible and interpreted their finding as evidence for the existence of vortex-like excitations above T_c [1] in line with a scenario in which phase-coherent superconductivity is destroyed above T_c due to the weakness of phase rigidity [13]. Our study, concentrated on the Nernst coefficient at high magnetic field leads to several new findings. First, a large Nernst signal was found to persist in presence of a field-induced non-metallic behavior in resistivity. This observation provides new support for the concept of vortices with insulating cores. Moreover, using both Nernst and resistivity data, we calculate the entropy associated with the vortex cores and compare it with the difference of entropy between the normal and superconducting states as extrapolated from specific heat studies [14]. Finally, we present the first set of data on the thermoelectric Hall angle and argue that its temperature-dependence (close to T^3) puts strong constraints on the origin of the residual Nernst signal above T_c first discovered by Xu *et al.* [1].

The preparation and characterisation of LSCO single crystals is described in detail elsewhere [15]. Our set-up was designed in a way to measure Seebeck and Nernst coefficients simultaneously as well as resistivity and Hall effect. The temperature profile along the sample was monitored by two miniature RuO_2 thermometers. Longitudinal and transverse DC voltages produced by this heat current were measured by two EM N11 Nanovoltmeters. The same contacts were used to measure electrical resistivity and Hall coefficient. A superconducting magnet was used for experiments up to 12 teslas whereas a Bitter magnet at Grenoble High Magnetic Field Laboratory was employed to access fields up to 28T.

Fig.1 shows the temperature-dependence of the Nernst signal and resistivity in a $\text{La}_{1.92}\text{Sr}_{0.08}\text{CuO}_4$ single crystal for various magnetic fields. In presence of a magnetic field of 12T, resistivity shows a broad transition ending at $T \sim 5\text{K}$. At the same field, we detect a large Nernst signal which peaks at $T \sim 18\text{K}$. Since the broad resistive transition is a consequence of dissipation due to the vortex movement, a concomitant Nernst signal due to the effect of a thermal force on the same vortices is naturally expected. This is in agreement with what has been reported in the case of optimally-doped cuprates [12]. However, the evolution of the Nernst signal at higher fields is surprising. As seen in the upper panel of Fig.1, a magnetic field of 26T is large enough to induce a slight non-metallic behavior in resistivity in the 15K-40K temperature range. However, at this field, the maximum in the Nernst signal occurs at almost the same temperature, broadens, and presents a reduced but still large magnitude. The coexistence of the peak in the Nernst signal with a non-metallic resistivity is in sharp contrast for what has been reported for all superconductors including optimally-doped cuprates [12]. It is the main new finding of this letter. This result is confirmed on two other single crystals at lower doping levels. Fig.2 shows the data on a $\text{La}_{1.94}\text{Sr}_{0.06}\text{CuO}_4$ single crystal. As seen in the figure, the sample shows a very broad resistive transition at zero field. The application of a magnetic field leads to the emergence of an insulating behavior, but barely affects the peak in the Nernst signal which, nevertheless, presents a reduced magnitude compared to the $x=0.08$ case. To reconcile the Nernst and resistivity data, it is tempting to assume that at high field, the system is populated by vortices which can move under the influence of a Lorentz force and produce a non-metallic resistivity. This may arise in the context of an insulating normal state, since the flux-flow resistivity, ρ_F is a fraction of the normal state resistivity ρ_N (in the simplest case $\frac{\rho_F}{\rho_N} \propto \frac{H}{H_{c2}}$ [16]). Thus, a non-metallic $\rho_F(T)$ may reflect the insulating behavior of $\rho_N(T)$ with attenuation.

More insight on the fuzzy phase-boundary between the superconducting and the normal states may be achieved by comparing the field-dependence of Nernst effect and resistivity of the $x=0.08$ sample. As seen in the upper panel of Fig.3, below T_c , Nernst coefficient is not a linear function of magnetic field. It presents a maximum which becomes broader at lower temperatures. Qualitatively, this behavior is understandable. The thermal force on each vortex is proportional to the excess of entropy associated with it. Since the latter would become zero at H_{c2} , the Nernst signal is expected to decrease at a finite field in spite of the increase in the number of vortices. As seen in the lower panel of Fig.3, the non-vanishing Nernst signal is concomitant with a large magnetoresistance up to the highest explored magnetic fields(28T). Extrapolating the Nernst data to higher magnetic fields, one can estimate that the signal would vanish at $H \sim 60\text{T}$ which is close to the estimation of H_{c2} deduced from

magnetoresistance saturation [2]. Fig.3 also displays the passage between metallic and non-metallic behaviors at $H \sim 27\text{T}$. It is worth noting that the magnitude of resistivity at the boundary between metallicity and non-metallicity ($0.39 \text{ m}\Omega\text{cm}$) yields a resistance close to $\frac{h}{4e^2}$ per CuO_2 plane, reported as the critical threshold resistance for superconductor-to-insulator transition in cuprates [3].

Combining the Nernst and resistivity data, one can calculate the entropy associated with these vortices [12]. When vortices move under the influence of a thermal force: $f_{th} = -\frac{\partial T}{\partial x} S_\phi$ (S_ϕ is the transport entropy per unit length of an individual vortex), they produce a transverse electric field according to the Josephson equation, $E_y = B_z v_x$, where v_x is the average vortex velocity. This velocity is proportional to the force applied on a vortex $v_x = \eta f_{th}$. with η being a viscosity coefficient. On the other hand, flux movement in presence of a Lorentz force on individual vortices, $f_L = J_x \Phi_0$, is at the origin of the longitudinal electric field produced by an electric current. $E_x = B_z v_y$. The same viscosity coefficient relates this velocity to the Lorentz force $v_y = \eta f_L$. Thus:

$$\frac{J_x \Phi_0 B_z}{E_x} = \frac{\frac{\partial T}{\partial x} S_\phi B_z}{E_y} \quad (1)$$

And defining resistivity as $\rho_F = \frac{E_x}{J_x}$ and the Nernst coefficient as $N = \frac{E_y}{\frac{\partial T}{\partial x}}$, one obtains [12]:

$$S_\phi = \frac{N \Phi_0}{\rho_F} \quad (2)$$

Now, the volume entropy at a given magnetic field is obtained by multiplying S_ϕ by $\frac{H}{\Phi_0}$, the density of the vortices at a given field H . Hence,

$$S_m = \frac{NH}{\rho_F V_m} \quad (3)$$

is the excess entropy carried by vortices at a given field in molar units. Here, V_m is the molar volume ($9.5 \cdot 10^{-29} \text{ m}^3/\text{mol}$ for LSCO [17]). Fig. 4 displays the temperature dependence of S_m obtained in this way for $H=12\text{T}$ and $H=26\text{T}$. In the picture sketched above, this plot represents the difference between the entropy accumulated by the vortices and the entropy of the background condensate.

As seen in the figure for both fields, S_m shows a maximum and remains finite well above $T_c (=27\text{K})$ in the ‘‘normal’’ state. This is a consequence of the finite value of Nernst coefficient above T_c and up to the highest temperature explored in this study ($\sim 63\text{K}$, see data in the lower panel of Fig.1). This latter observation, first reported by Xu *et al.* [1] was interpreted by these authors as evidence for vortex-like excitations in the pseudo-gap regime. So, the analysis sketched above leads to the existence of a substantial S_m persisting upto T^* [1] (the temperature below which the pseudo-gap opens up). Note that this

simple analysis remains valid for any exotic electronic excitation which happens to be a reservoir of entropy (in order to move by a thermal gradient) and either a topological defect in a phase-coherent environment or a fluxoid (in order to produce an electric field by its movement). As indicated by the absence of Φ_0 in equation (3), it should not necessarily be associated with a single flux quantum (i.e. a standard Abrikosov vortex). Note, however, that while below $T_c(H=0)$, the resistivity is entirely generated by the vortex movement and there is no ambiguity about the magnitude of ρ_F , this is not the case in the normal state. Indeed, at this stage, in the absence of any solid evidence for vortex dissipation in charge transport, the magnitude of ρ_F above T_c is a matter of speculation. On the other hand, our estimation of S_m in the superconducting state is straightforward and does not suffer from the current uncertainty on the origin of the residual Nernst signal in the pseudo-gap regime.

It is interesting to compare the temperature dependence and the magnitude of S_m with the results of the extensive study of specific heat in cuprates by Loram *et al.* [14]. Besides its finite value above T_c , the overall temperature dependence of $S_m(T)$ is reminiscent of the difference between the entropy of the superconducting state and the extrapolated entropy of the “normal” state obtained by specific heat measurements. However, the magnitude of S_m is almost an order of magnitude smaller than the maximum in the difference in the specific heat data for LSCO at this doping level [14]. The discrepancy is probably due to the important differences between the nature of information obtained by these two probes. First of all, our results are obtained in presence of a strong magnetic field which is known to diminish and broaden the electronic specific heat jump and consequently reduce the entropy difference between the two states [18]. In the second place, the transport entropy of (i.e. the entropy carried by) a vortex is yet to be theoretically clarified in the context of d-wave superconductivity. To the first approximation, the electronic excitation spectrum of the vortex core (defined as the region within a coherence length of the center) reflects that of the normal state. STM studies of the high- T_c cuprates [9,10], however, have reported a remarkably reduced difference in the low-energy Density Of States inside and far away from vortex cores compared to what has been observed in a conventional superconductor [19].

Finally, let us consider possible alternative origins of the observed Nernst signal above T_c . Since vortex movement is not the only source of a Nernst signal, it is useful to underline the restrictions that a quasiparticle scenario should face in order to account for such a signal in our context. For this purpose, we used our set-up to measure the ratio of the longitudinal to transverse electric fields produced by a fixed thermal current, \vec{J}_q , along the sample. This ratio directly determines the field-induced rotation of the electric field produced by a thermal current. The cotangent of the thermoelectric Hall angle, $\cot \theta_{HTE}$, obtained in this way may be compared with the electric

Hall angle, $\cot \theta_H$. The lower panel of Fig.4 compares the evolution of the two angles. As seen in the figure, the thermoelectric Hall angle presents a T^3 behavior in the “normal” state and becomes even stronger (and field-dependent) below T_c . This reflects the rapid increase in the Nernst signal below T^* and its non-linearity below T_c . In the same temperature region, the measured electric Hall angle is almost temperature-independent. [For LSCO at this doping level, the quadratic term in $\cot \theta_H$ is very small at our temperature range [21]]. Now, $\vec{J}_q = \bar{\alpha} \vec{E} + \bar{\kappa} \vec{\nabla} T$ and, since there is no charge current, $\vec{\sigma} \vec{E} = \frac{\bar{\sigma}}{T} \vec{\nabla} T$ which yields $\vec{J}_q = (\bar{\alpha} + \bar{\kappa} \bar{\alpha}^{-1} \bar{\sigma} T) \vec{E}$ (see the inset of Fig. 1). Therefore the angle between \vec{J}_q and \vec{E} reflects the rotations produced by $\bar{\alpha}$, $\bar{\kappa}$ and $\bar{\sigma}$ which are the thermoelectric, thermal and electric conductivity tensors. Explaining the rapid temperature-dependence of $\cot \theta_{HTE}$ seems to be a major challenge for the standard transport theory. Indeed, it has already been noted that in absence of an energy-dependence in the scattering time, $\tau(\epsilon)$, and even for a highly anisotropic single Fermi surface, the two ratios $\frac{\alpha_{xx}}{\alpha_{xy}}$ and $\frac{\sigma_{xx}}{\sigma_{xy}}$ are expected to be equal [22] which implies an identical rotation due to $\bar{\alpha}$ and $\bar{\sigma}$. More generally, in a Boltzmann picture [20]:

$$\bar{\alpha} = \frac{(\pi k_B T)^2}{3} \frac{\partial \bar{\sigma}}{\partial \epsilon} \Big|_{\epsilon=\epsilon_F} \quad (4)$$

which establishes an intimate relationship between the two angles even in the case of a highly energy-dependent $\tau(\epsilon)$. Any alternative scenario on the origin of the finite Nernst signal above T_c implying quasiparticles instead of vortices is expected to explain the contrasting behavior of the two angles. We note that equation(4) is only valid when charge and entropy are carried by the same electronic excitations which is not the case in the charge-spin separation scenarios.

In summary, we studied Nernst effect at high magnetic fields in underdoped LSCO and found that the Nernst signal persists in presence of a magnetically-induced non-metallic behavior. We extracted the entropy carried by vortices in the vicinity of this superconductor-to-insulator transition and measured the temperature-dependence of the thermoelectric Hall angle. This work was supported by the Förderung der wissenschaftlichen Forschung of Austria, the Franco-Austrian Amadeus program and by the Fondation Langlois.

-
- [1] Z. A. Xu *et al.*, Nature **406**, 486 (2000).
 - [2] Y. Ando *et al.*, Phys. Rev. Lett. **75**, 4662(1995); G. Boebinger *et al.*, Phys. Rev. Lett. **77**, 5417 (1996); S. Ono *et al.*, Phys. Rev. Lett. **85**, 638 (2000).
 - [3] K. Semba and A. Matsuda, Phys. Rev. Lett. **86**, 496 (2001).

- [4] Y. Fukuzumi *et al.*, Phys. Rev. Lett. **76**, 684 (1996).
 [5] D. P. Arovas *et al.*, Phys. Rev. Lett. **79**, 2871 (1997).
 [6] J. H. Han and D-H. Lee, Phys. Rev. Lett. **85**, 1100 (2000).
 [7] M. Franz and Z. Tesanovic, Phys. Rev. B **63**, 064516 (2001).
 [8] B. Lake *et al.*, Science **291**, 1759 (2001); cond-mat/0104026 (2001).
 [9] S. H. Pan *et al.*, Phys. Rev. Lett. **85**, 1536 (2000).
 [10] I. Maggio-Aprile *et al.*, Phys. Rev. Lett. **75**, 2754 (1995); B. W. Hoogenboom *et al.*, cond-mat/0105528 (2001).
 [11] K. Kappinska *et al.*, Phys. Rev. Lett. **77**, 3033 (1996); A. Malinowski *et al.*, Phys. Rev. Lett. **79**, 495 (1997).
 [12] H.-C. Ri *et al.*, Phys. Rev. B **50**, 3312 (1994).
 [13] V. J. Emery and S. A. Kivelson, Nature **374**, 434 (1995).
 [14] J. W. Loram *et al.*, J. Phys. Chem. Solids **59**, 2091 (1998).
 [15] Ch. Marin *et al.*, Physica C **320**, 197 (1999).
 [16] J. Bardeen and M. J. Stephen, Physical Review **140**, A1197(1965).
 [17] D. A. Harshman and A. P. Mills, Jr., Phys. Rev. B **45**, 10684 (1992).
 [18] A. Junod *et al.*, Physica C **275**, 245(1997).
 [19] H. F. Hess *et al.*, Phys. Rev. Lett. **62**, 214 (1989).
 [20] J. M. Ziman, Principles of the theory of solids, Cambridge University Press (1972).
 [21] F. F. Balakirev *et al.*, Phys. Rev. B **57**, R8083 (1998).
 [22] J. Clayhold Phys. Rev. B **54**, 6103(1996).

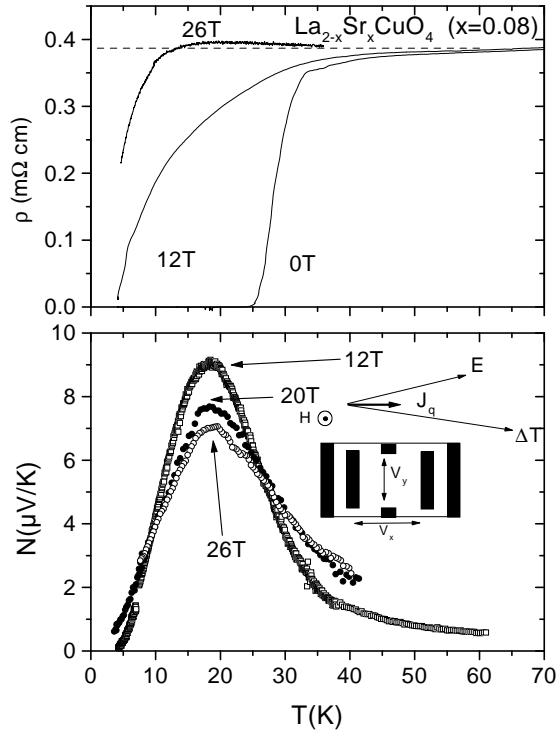


FIG. 1. Resistivity and Nernst effect as a function of temperature in an underdoped LSCO crystal for different magnetic fields. The broken horizontal line represents $0.39 m\Omega cm$. Inset shows the contact geometry on the sample and the relevant vectors.

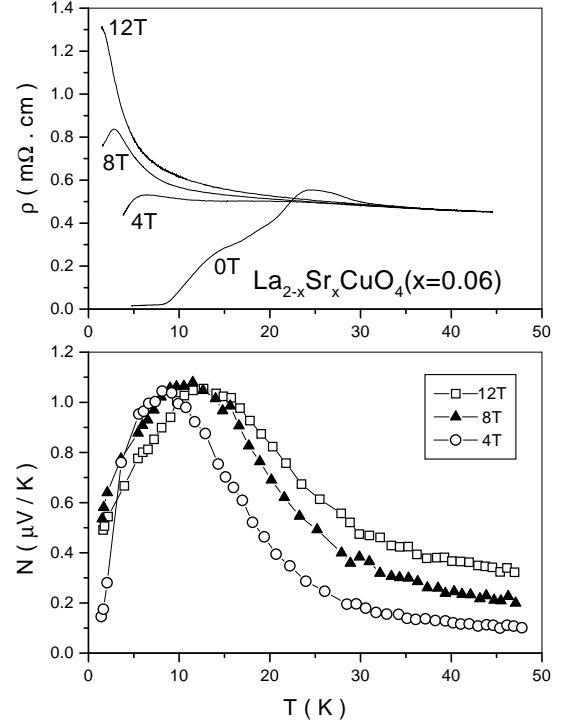


FIG. 2. Resistivity and Nernst effect as a function of temperature in another underdoped LSCO crystal for different magnetic fields. Note the coexistence of a Nernst signal and an apparently insulating behavior at $H=12T$.

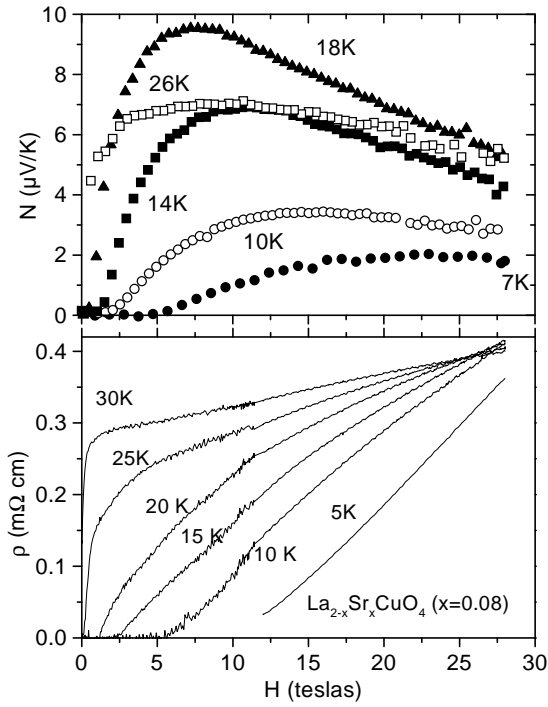


FIG. 3. Resistivity and Nernst effect as a function of field in an underdoped LSCO crystal for different temperatures.

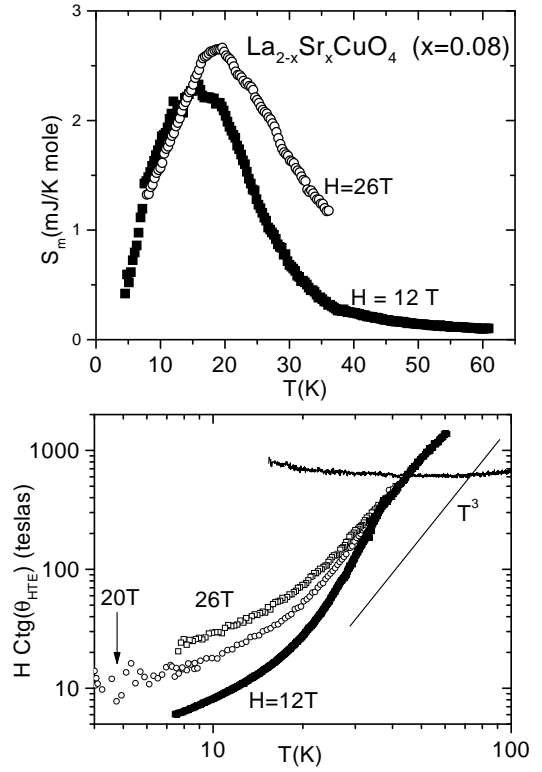


FIG. 4. Upper panel: Entropy carried by vortices as extracted from resistivity and Nernst coefficient for the $x=0.08$ sample at two different magnetic fields (See text). Lower Panel: The temperature dependence of the normalized thermoelectric Hall angle at different magnetic fields. The solid line represents the normalised electric Hall angle (measured at 12 T) for the same sample.